



Limitations of $Sa(T_1)$ as an intensity measure when assessing non-ductile infilled RC frame structures

Gerard J. O'Reilly¹

Received: 12 December 2020 / Accepted: 27 February 2021 / Published online: 12 March 2021
© The Author(s), under exclusive licence to Springer Nature B.V. 2021

Abstract

An important decision in seismic risk assessment involves a good choice of intensity measure (IM) used to describe ground motion intensity. Depending on the structural typology and type of analysis, the choice of an optimal IM may differ. Ideally, it should have accurate response predictions and not be biased by parameters like scaling factors or other ground motion characteristics. This article investigates this topic in the context of non-ductile reinforced concrete (RC) frames with masonry infills. It examines several case study structures with IMs like peak ground acceleration (*PGA*), peak ground velocity (*PGV*), first mode spectral acceleration, $Sa(T_1)$, and average spectral acceleration, *AvgSa*. It reveals *PGA* and *PGV* to possess undesirable traits relating to inefficiency, sensitivity to scaling and dependence on other ground motion parameters. $Sa(T_1)$ is shown to be an optimal IM at lower intensities, but runs into difficulty once the infill panels collapse and a non-ductile mechanism forms in the structure. Further investigation shows that the response is strongly biased by the velocity-based characteristics of the record upon infill panel collapse when using $Sa(T_1)$. On the other hand, *AvgSa* is seen to possess many of the same benefits regarding efficient response prediction for both intensity-based assessment and fragility function development but is not biased by the ground motion velocity-based characteristics. In light of this, this study presents a case for the traditional IM $Sa(T_1)$ to be set aside and for a more promising alternative in *AvgSa* to be adopted when analysing existing infilled RC frames.

Keywords PBEE · Fragility · Intensity measure · Bias · Assessment

1 Introduction

Seismic risk assessment involves the estimation of seismic damage in structures and infrastructures. Their accuracy is thus critical in reducing and managing seismic risk as part of what is generally termed performance-based earthquake engineering (PBEE) (Cornell and Krawinkler 2000). PBEE describes, in part, monetary losses (direct and indirect) and loss of life in a probabilistic manner due to ground shaking. To this end, engineers utilise distinct indicators, or limit states, to describe performance in quantifiable terms. For example,

✉ Gerard J. O'Reilly
gerard.oreilly@iusspavia.it

¹ Scuola Universitaria Superiore IUSS Pavia, Piazza della Vittoria 15, 27100 Pavia, Italy

the collapse of a structure, which would result in the casualty of its occupants, can be quantified using analysis procedures like incremental dynamic analysis (IDA) (Vamvatsikos and Cornell 2002) or multiple stripe analysis (MSA) (Jalayer and Cornell 2009; Jalayer 2003). Likewise, FEMA P-58 (FEMA 2012) can be used to estimate the expected monetary losses due to structural and non-structural damage in buildings whilst also dealing with consequences like expected downtime. These methodologies seek to quantify these limit states via the level of ground shaking needed to induce them.

An intensity measure (IM) is the interface parameter linking seismological and engineering aspects in seismic design and assessment. Ground motion prediction equations (GMPEs) are used as part of probabilistic seismic hazard analysis (PSHA) to evaluate the probability of exceeding an IM level for a specific location over a given period of time. Engineers then use the same IM to examine the subsequent response of structures and to evaluate seismic response. Past research on the topic notes that a desirable IM ought to be efficient, sufficient and hazard computability. Hazard computability ensures that it is feasible to carry out PSHA with a suitable library of GMPEs and available tools to obtain a hazard curve needed to compute risk. Efficiency implies that the structural response should exhibit relatively low dispersion for the response parameters of interest. Lastly, sufficiency means that the analysis results obtained are independent of any other ground motion rupture parameters.

Within the PBEE framework, a desirable characteristic of an IM is for it to be a good descriptor of structural response (i.e. efficient). Furthermore, it is implied that other parameters do not have a notable influence, or bias, on the response estimates. For example, the spectral acceleration at the first mode period, $Sa(T_1)$, of a structure dominated by first mode response tends to be a good descriptor of the displacement response, whereas peak ground acceleration (*PGA*) is better linked to the absolute floor accelerations observed. An example of potential bias would be the study by Chandramohan et al. (2016) who, when investigating the impacts of ground motion duration on the collapse capacity of degrading systems when using $Sa(T_1)$ as the IM, showed that spectrally equivalent records with longer duration tended to be more aggressive compared to shorter duration records, illustrating the potential bias if duration is neglected.

There have been several past studies (Minas and Galasso 2019; Silva et al. 2019; Jalayer et al. 2012; Padgett et al. 2008; Mehanny 2009; Giovenale et al. 2004; Kohrangi et al. 2016) examining IMs for different structural typologies in order to identify the benefits and drawbacks of each in various contexts. For example, a study by Minas and Galasso (2019) investigated ways in which displacement-based demands could be more accurately estimated for mid-rise reinforced concrete (RC) frames using different IMs. Another study by Padgett et al. (2008) examined the selection of optimal intensity measures to be used in probabilistic seismic demand models when assessing highway bridge portfolios. When it comes to the assessment of existing infilled RC frames in particular, some caveats arise. Several studies have examined their seismic vulnerability or fragility using IMs like $Sa(T)$ (Villar-Vega et al. 2017; Rossetto and Elnashai 2003), *PGA* (Agudelo and López 2009; Borzi et al. 2008; Kappos et al. 2003; Villar-Vega et al. 2017; HAZUS 2003; Del Gaudio et al. 2017; Lagomarsino and Giovinazzi 2006; Rota et al. 2008) or peak ground velocity (*PGV*) (Erberik 2008; Akkar et al. 2005). These are relatively simple IMs that can be adopted for regional studies, evident through their implementation and availability in OpenQuake engine's risk toolkit (Silva et al. 2015), for example. *PGA* has been used quite consistently in the development of empirical fragility functions using data from past events (Del Gaudio et al. 2017; Rossetto and Elnashai 2003; Rota et al. 2008; Del Gaudio et al. 2019a, b), likely due to its simplicity and convenience when homogenising data,

which is also an advantage of *PGV*. Rossetto and Elnashai (2003), however, noted that *PGA* was quite a poor predictor of damage when compared to other spectral-based IMs, noting the lack of consideration of structural dynamic properties or site geology, amongst other issues. This limitation was noted as a primary reason for underprediction of structural damage when *PGA*-based fragility curves were evaluated.

When using $Sa(T_1)$, the elongation of the first mode period of vibration, T_1 , due to the local collapse of infill walls that may result in significant strength degradation and subsequent period elongation before the eventual global collapse is of notable importance. The shift in modal properties means that an IM anchored to the initial period of the undamaged structure can be rather inefficient when assessing non-linear behaviour. T_1 is herein used to describe the initial period of vibration of the undamaged structure that a numerical model would report, and not any other period computed via a secant-to-yield stiffness or stiffness following the cracking of infill panels or slight damage to RC members. In fact, Kazantzi and Vamvatsikos (2015) noted that when a structure has formed and settled into a damage mechanism, it tends to behave closer to a structure with an elongated first-mode period, and consideration of this elongated period greatly improves the efficiency and sufficiency of the $Sa(T)$ -based IM. Hence, the consideration of periods other than the undamaged first mode period in IM definition is examined here.

This study focusses on IMs to characterise the response of non-ductile RC frames with masonry infills, a typology widely constructed prior to the introduction of modern design codes in the Southern Mediterranean area. It aims to identify a simple and efficient IM for such structures that satisfies the desirable IM characteristics in seismic assessment, particularly related to improved efficiency and reduced bias in results. Several case study structures are analysed for a site in Italy using different IM definitions. Results are evaluated in terms of their sufficiency and efficiency. Bias was examined to identify other ground motion parameters potentially influencing response to provide a further understanding on the particularities of such a structural system when it comes to seismic assessment.

2 Case study structures

Fifteen RC frame typologies designed for gravity loads only were adopted from a past study (O'Reilly and Sullivan 2018a). They are representative of RC frame structures built in Italy before the introduction of modern seismic design code provisions around the 1970s. The frames were numerically modelled using OpenSees (McKenna et al. 2010) adopting the modelling approach of O'Reilly and Sullivan (2019) for the various structural elements characteristic of these non-ductile infilled RC frames. In particular, lumped plasticity elements were used to model the beam and column elements, using available experimental test data on both sub-assemblies and building specimens to quantify the various modelling parameters for older RC frames. Equivalent diagonal strut models (Crisafulli et al. 2000) were adopted to incorporate the effects of masonry infill along with the proposals of Sassun et al. (2015) and Hak et al. (2012) for the hysteretic backbone of these struts. Beam-column joints were modelled using a zero-length hinge at the joint centres to characterise the vulnerability to brittle shear failure as a result of little to no transverse reinforcement in this region, following the modelling approach outlined in O'Reilly and Sullivan (2019). Three different combinations of masonry infill were also considered, termed: *weak*; *medium*; and *strong* infill, defined and modelled using the infill strength properties described in Hak et al. (2012) and deformation parameters based on experimental test data in Sassun et al.

(2015), and were modelled as uniformly distributed over the height of the structure. Since the strength was a function of the masonry typology but the deformation parameters were assumed constant, the relative stiffness of the infill was indirectly accounted for between infill typologies. Furthermore, the additional self-weight of the masonry infill panels was considered as a lumped mass at each supporting beam end for simplicity, and was computed as a function of the infill panel's unit weight. The structural details and modal properties (i.e. periods, T and percentage modal mass, M) are listed in Table 1.

3 Intensity measures

To examine the seismic response characterisation of infilled RC structures, several IMs were adopted. The impacts of these choices on the seismic vulnerability characterisation, namely in terms of the response characterisation efficiency and potential bias, will be then discussed in later sections. The IMs adopted were:

- PGA —defined as the peak ground acceleration of a given ground motion record;
- $Sa(T_1)$ —the 5%-damped pseudo-spectral acceleration at T_1 of a given structure;
- PGV —defined as the peak ground velocity of a given record;
- $AvgSa$ —the average spectral acceleration spanning T_{lower} and T_{upper} of a given record.

PGA and PGV are self-explanatory quantities and simply define the absolute peak of the ground acceleration and velocity, respectively, with no connection to a structure's dynamic properties. $Sa(T_1)$ corresponds to the spectral acceleration at the first mode period of vibration for each structure. For $AvgSa$, the geometric mean of the $Sa(T)$ values in the period range $[T_{lower}, T_{upper}]$ with a spacing of 0.1 s was utilised. This spacing was chosen as it corresponds to a value below which the estimate of $AvgSa$ for a given record was observed to stabilise, since the value of $AvgSa$ is sensitive to the spacing between the periods used if too large. Therefore a spacing of 0.1 s is recommended but it is noted that the hazard analysis for an extremely small spacing can become computationally demanding so very small spacings should be avoided.

Kazantzi and Vamvatsikos (2015), followed by Kohrangi et al. (2017), interchangeably used ranges of $[T_{lower}, T_{upper}]$ equal to $[0.2T_1, 1.5T_1]$ or $[T_2, 1.5T_1]$ for $AvgSa$ when examining ductile RC frames without masonry infills. It is important to consider the elongation of a structure's fundamental period, as it has been noted to be a relevant parameter in non-linear structural response towards collapse. By taking the elongation of an infilled RC frames' first mode period once the infill panels have been damaged to be approximately double (O'Reilly et al. 2018a), a more suitable period range covering the likely modal properties is defined here for $AvgSa$. The period of the damaged structure, as opposed to the completely bare frame period, is used based on the work of Nafeh et al. (2020). The damaged structure in this context implies the structure with the struts used to model the infill removed at the storey where the mechanism is expected to develop from a pushover analysis. Nafeh et al. (2020) found that once the infill panels become damage and collapse at a single storey, the dynamic properties of the structure from that point onwards tend to be more in line with this damaged structure as opposed to a completely bare frame, which tended to notable overestimate the flexibility of the frame. Further details can be found in Sect. 2.2 of Nafeh et al. (2020).

Table 1 Description of case study structural configurations, modal properties and IM definition

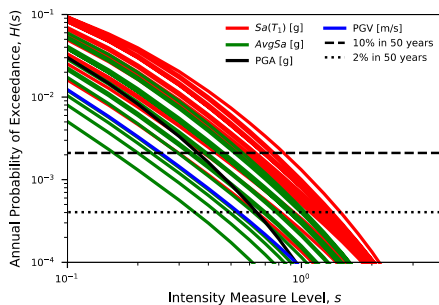
Structural Configuration			Modal properties					IM definition				
ID	# Storeys	Masonry Typology	T_1 [s]	T_2 [s]	T_3 [s]	M_1 [%]	M_2 [%]	M_3 [%]	ΣM [%]	$Sa(T_1)$	T_{lower} [s]	T_{upper} [s]
RC-WI-2	2	Weak	0.248	0.103	–	86	14	–	100	0.25	0.12	0.74
RC-WI-3	3	Weak	0.369	0.135	0.098	83	11	5	100	0.37	0.16	1.11
RC-WI-4	4	Weak	0.444	0.164	0.109	81	14	2	97	0.44	0.20	1.33
RC-WI-6	6	Weak	0.627	0.230	0.142	79	15	3	96	0.63	0.28	1.88
RC-WI-9	9	Weak	0.927	0.334	0.192	76	14	3	94	0.93	0.40	2.78
RC-MI-2	2	Medium	0.192	0.080	–	86	14	–	100	0.19	0.10	0.58
RC-MI-3	3	Medium	0.287	0.105	0.076	83	12	5	100	0.29	0.13	0.86
RC-MI-4	4	Medium	0.349	0.128	0.085	81	14	2	98	0.35	0.15	1.05
RC-MI-6	6	Medium	0.482	0.178	0.104	81	13	4	97	0.48	0.21	1.45
RC-MI-9	9	Medium	0.744	0.264	0.147	77	14	4	95	0.74	0.32	2.23
RC-SI-2	2	Strong	0.154	0.064	–	86	14	–	100	0.15	0.08	0.46
RC-SI-3	3	Strong	0.209	0.084	0.053	86	11	3	100	0.21	0.10	0.63
RC-SI-4	4	Strong	0.288	0.107	0.070	81	15	2	98	0.29	0.13	0.86
RC-SI-6	6	Strong	0.414	0.151	0.087	80	13	4	97	0.41	0.18	1.24
RC-SI-9	9	Strong	0.653	0.227	0.124	76	15	4	96	0.65	0.27	1.96

Combining this primary source of period elongation with the further elongation due to the RC frame damage gives $T_{upper} = 1.5 \cdot (2T_1) = 3T_1$ being proposed. For T_{lower} , the second mode period was analysed in a similar fashion, where the lower limit of T_2 used by Kazantzi and Vamvatsikos (2015) was adopted, and following a similar analysis by O’Reilly et al. (2018a) into the impact of infill panel damage on the second mode of vibration, it was found to increase by approximately 20%, giving $T_{lower} = 1.2T_2$. This consideration of periods lower than the first mode stems from past work by Eads et al. (2016), among others, who noted the benefits of including spectral values at periods lower than T_1 compared to other studies like Bojórquez and Iervolino (2011), for example, who considered the elongation from the first mode period only. Therefore, a period range of $[1.2T_2, 3T_1]$ is proposed as the *AvgSa* period range for infilled RC frames. Table 1 lists the information utilised for the IM definition.

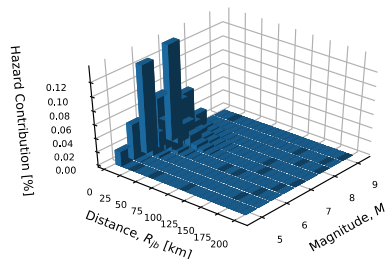
4 Hazard and ground motions

PSHA was carried out for a site in L’Aquila, Italy using the OpenQuake engine (GEM 2019) developed by the GEM Foundation and the SHARE hazard model (Woessner et al. 2015). This site was chosen as it represents a moderately high seismicity site in the Mediterranean area that was heavily damaged during the 2009 earthquake (Ricci et al. 2011). As will be seen in later sections, velocity-based characteristics of ground motions will be discussed for the case study structures presented. Since the chosen site of L’Aquila has no particular features that may lead to large velocity or other notable characteristics (e.g. directivity effects), the findings presented herein are expected to be generally applicable to other sites in the Mediterranean area for these non-ductile infilled RC frames.

It is important to note that the option to do hazard analysis with *AvgSa* as the IM has been recently added to the OpenQuake engine, meaning that it’s hazard curve calculation is just as obtainable as any other IM examined here. A V_{s30} of 300 m/s corresponding to stiff clay was adopted and site hazard curves describing the annual probability of exceedance, H , for a given IM level, s , were quantified for each IM, as shown in Fig. 1a. The relative contribution of different causal rupture characteristics (i.e. disaggregation) to each IM’s hazard curve was also identified (Fig. 1b).



(a) Hazard curves obtained for each IM examined



(b) Disaggregation of $Sa(T=0.37s)$ for the 10% probability of exceedance in 50 years hazard level

Fig. 1 Illustration of the PSHA results obtained for a site in L’Aquila, Italy

For each IM examined, 40 ground motion records were selected for discrete intensity levels to carry out MSA and characterise the structural response with increasing intensity. For the $Sa(T)$ -based IMs, the conditional spectrum (CS) approach by Baker (2011) was followed, whereas its extension to $AvgSa$ -based selection by Kohrangi et al. (2017) was used. The correlation model by Baker and Jayaram (2008) was used in both cases. CS-based approaches were not used for PGA and PGV . In these cases, records with rupture characteristics compatible with the mean PSHA disaggregation were selected and scaled for each intensity level. This was to replicate a more casual record selection adopted for such IMs, where suitable records are identified based on rupture parameters and conditional hazard approaches are generally not considered. Twelve intensity levels were investigated, corresponding to probabilities of exceedance ranging from 90 to 0.1% in 50 years, ensuring that the structural response covering initial damage of the masonry infill panels right up to global structural collapse could be characterised. Figure 2 shows an example ground motion selection for both $Sa(T)$ and $AvgSa$. In all cases, records with directivity-induced velocity pulses were not utilised.

Furthermore, for each IM and structure investigated, an additional set of 60 ground motion records were selected using the hazard information at the 2% in 50 years hazard level (i.e. 2475 year return period) to also perform IDA (Vamvatsikos and Cornell 2002). IDA was conducted so that the intensity causing collapse for a series of records could be estimated. MSA does not provide this kind of output since the records are selected for a

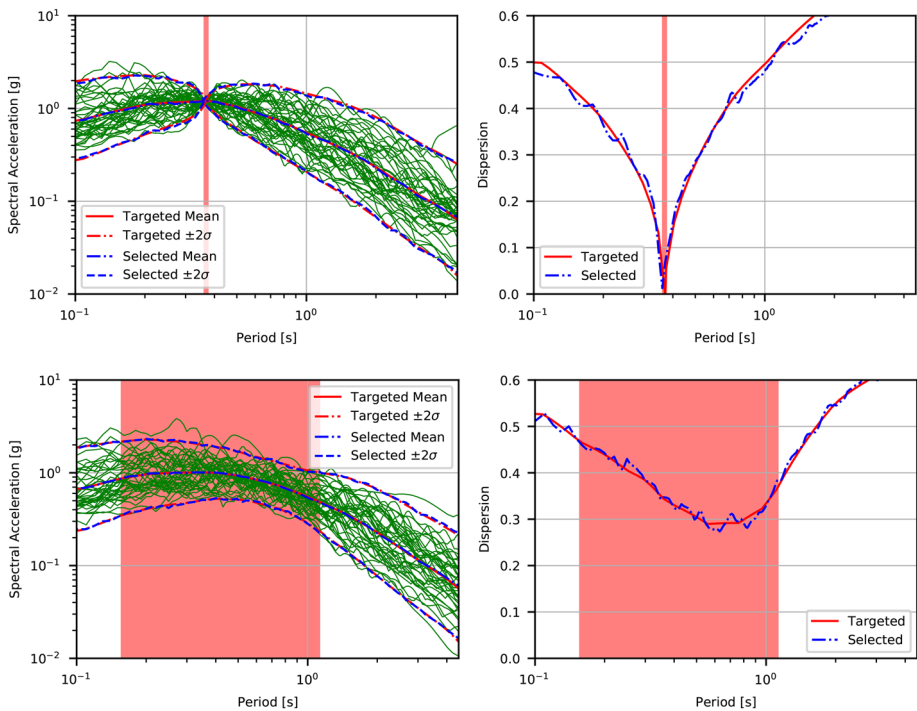


Fig. 2 Set of 40 ground motion records selected for the RC-WI-3 structure at the 2% in 50 years probability of exceedance for (top) $Sa(T_1 = 0.37 \text{ s})$ and (bottom) $AvgSa$, where matching of the selected mean and dispersion is compared to the targeted distribution. The red shaded zones indicate the conditioning period value (or range) used

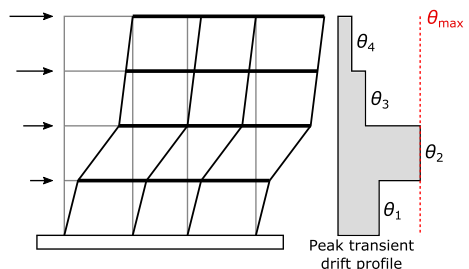
number of return period stripes. Collapse cases in MSA are described in a pass/fail manner, without any information about the intensity that induced collapse for a given record. This information will be needed to briefly analyse the collapse cases sufficiency, which is discussed in Sect. 7.2.

5 Characterisation of structural response

When characterising the structural response with increasing seismic intensity, a representative engineering demand parameter (EDP) is identified. In buildings, roof or storey drift ratio are common, since they characterise the response of first mode dominated structures quite well. Therefore, the maximum of the peak transient storey drifts along the building height, θ_{\max} , was adopted as the EDP (Fig. 3). To describe the structural performance via θ_{\max} , three limit states were identified: 0.18%, 1.0% and lateral structural collapse. A value of $\theta_{\max} = 5\%$ was adopted for collapse based on the findings of O'Reilly et al. (2018c). The limit of 0.18% was chosen since this is the drift at which the masonry infills were modelled as having cracked and lost a considerable amount of strength and stiffness, as per Sassun et al. (2015). This is a simplified definition of the cracking limit state, as it intends to be consistent with the numerical modelling strategy adopted for all infill typologies. A further refinement of this limit state definition as a function of infill typology may be implemented in more detailed studies using the work of Del Gaudio et al. (2019a, b) or Morandi et al. (2018), for example. This limit has been previously highlighted (O'Reilly and Monteiro 2019) as being rather critical when quantifying the performance of infilled RC frame structures. The limit of 1.0% was chosen to describe a level of demand that could be associated with non-linear RC frame response. For the case study structures examined here, yield storey drifts (assuming a column mechanism) ranged between 0.60 and 0.91% following the approach of Glaister and Pinho (2003). It is noted that these limit states are not intended to be used in place of more refined data in more specific studies, but rather general demand thresholds upon which different performance ranges of the case study structures could be characterised in order to collectively compare the different intensity measures examined.

As shown in Fig. 3, the current study focusses on 2D planar frames to investigate the relative performance of different IMs. Past studies on existing school buildings in Italy with the same structural typology (i.e. non-ductile infilled RC frames) have been conducted using a similar modelling approach to the one adopted here but for complete 3D structures using detailed survey information gathered in-situ (O'Reilly et al. 2018b; Carofilis et al. 2020). For those existing buildings, static pushover analysis also showed the same notable impact of the masonry infills with respect to the bare frames (i.e. significant increase in stiffness and strength initially followed by a drop), which was also recently discussed in

Fig. 3 Definition of maximum peak storey drift used as the EDP in dynamic analysis



detail by Nafeh et al. (2020). Furthermore, a comparison of the modal properties of the numerical models developed with ambient vibration and seismically triggered vibration during the 2016 Central Italy earthquakes in O’Reilly et al. (2019) showed the importance and relevance of the period elongation as a result of damage to the RC beam and column members as well as the masonry infill panels. Based on these observations, it is expected that the findings presented in this present study regarding IM efficiency and potential bias are also applicable to 3D structures typically encountered.

6 Analysis results

6.1 MSA results

MSA was carried out for each case study structure with each set of 40 ground motion records selected for the 12 return periods and 4 IMs described previously in Sect. 4. Figure 4 illustrates a representative example of the results obtained. It shows the individual response points for each record alongside the median, 16% and 84% fractiles for the non-collapse cases. The collapse cases are marked for each intensity in the right-hand side plot alongside the fitted collapse fragility function. This was fitted using the maximum

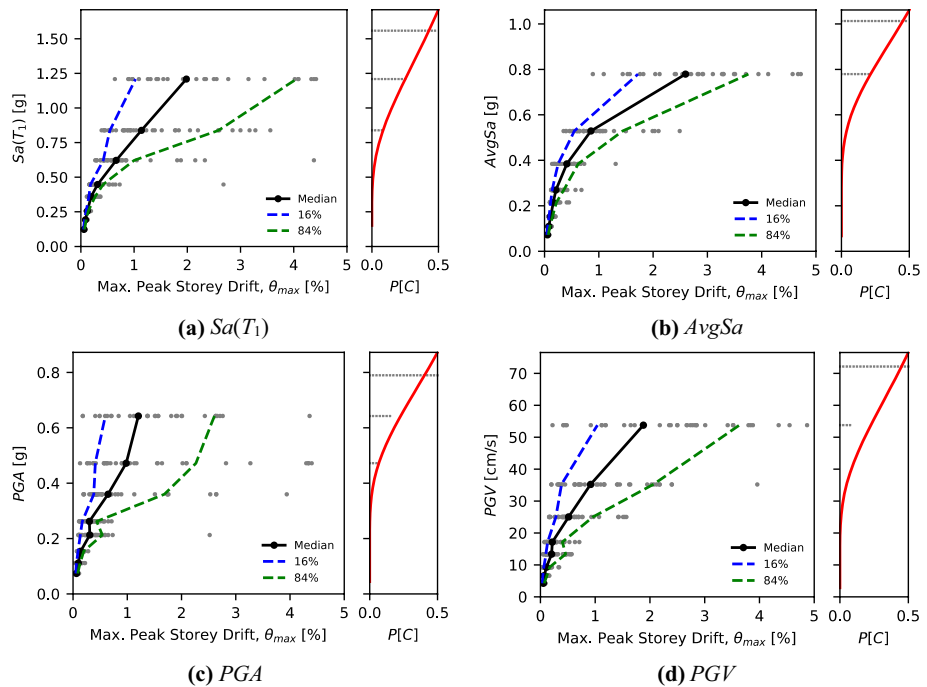


Fig. 4 MSA results for the 3 storey structure with weak infills (RC-WI-3) for the 4 IMs investigated. Note: each subplot shows (left) the response at each intensity level (or return period) with $P[C] < 50\%$ via the grey markers in addition to the 50% (median), 16% and 84% fractiles for the non-collapse cases and (right) the collapse cases observed at each intensity with the fitted lognormal distribution shown in red

likelihood method, whereby the fraction of collapses at each intensity measure level (IML) was used to fit a suitable continuous lognormal distribution.

The θ_{max} demand evolution in the structure in Fig. 4 tends to be relatively low and tightly bound for lower intensities, but quickly accumulates for higher intensities. This has been noted in past work (O’Reilly and Monteiro 2019; Nafeh et al. 2020) to result from the characteristic response of infilled RC frames. Initially, the structure behaves in a somewhat typical, first mode-based manner, with demands distributed along the height. Upon damage and collapse of the masonry infill panels in one or more storeys due to its non-ductile behaviour, a significantly modified dynamic response results thereafter, observed by the concentration of damage in the weaker storey(s), which is reflected via its period elongation. Also of note is the relative magnitude of the dispersion in results between the different IMs. This dispersion in the EDP is a function of the record-to-record variability, the IM used to characterise the response and also the location of the non-ductile mechanism in the structure. This last source derives from the definition of the EDP used for the structures (Fig. 3) as the maximum value along the height, meaning that the dispersion may increase should different ground motion records activate collapsing mechanisms at different storeys. Inspecting the location of the non-ductile mechanisms in the case study structures did not show any notable variations between ground motions and IMs and were seen to be relatively consistent for each respective structure heights and infill typology. This would imply that the additional source of uncertainty due to the collapse mechanism being located at different storeys was not significant compared to the other sources examined here. Assuming the data are lognormally distributed, meaning the random variable under consideration is the EDP value at a given IML, Fig. 5 plots this dispersion in demand for a given IML, $\beta_{EDPIIML}$, for each IM. The lognormality was checked using the Kolmogorov–Smirnov goodness of fit test at the 5% significance level and was general found to be satisfactory. From a total of 720 cases (i.e. 5 heights, 3 typologies, 4 IMs, 12 IMLs), the test hypothesis that the data follows a lognormal distribution was rejected in just 25 (3.5%) instances. Further scrutiny of these rejected instances did not reveal any obvious relationship between them and the presence of collapse cases or activation of other response mechanisms (i.e. the maximum value not always being recorded at the same storey level).

In Fig. 5, *PGA* and *PGV* exhibit the highest $\beta_{EDPIIML}$ initially and progressively increase with T_R . This is an expected result since these IMs have no direct relationship with respect to the structural dynamic properties. *Sa(T₁)*, on the other hand, exhibits the best predictive power for lower intensity levels, seen through its low $\beta_{EDPIIML}$. This is expected given its

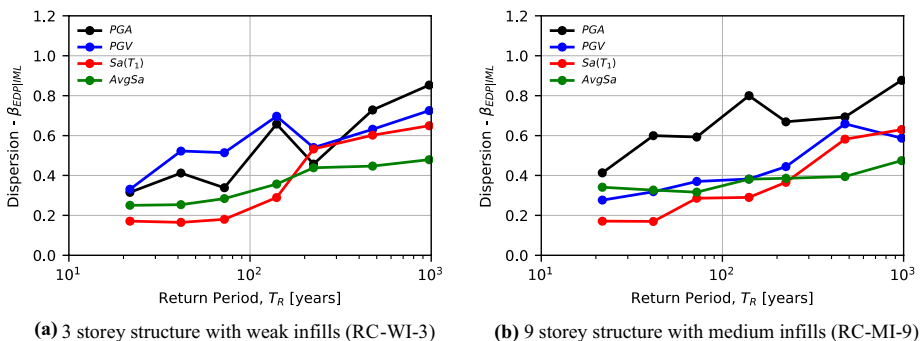


Fig. 5 Example of the dispersion in demand, $\beta_{EDPIIML}$ versus return period, T_R , for the IMs investigated

close relationship with deformation-based EDPs of structures with a dominant first mode responding in the elastic range. Past studies (Lin et al. 2013; Haselton and Baker 2006; Bradley et al. 2009) have also shown $Sa(T_1)$ to be a good predictor of structural response during elastic response, but that it loses its efficiency when the structure is responding well into the non-linear range of response. This is also evident in Fig. 5 through the sharp rise in $\beta_{EDPIIML}$ for higher T_R .

Period elongation is of notable importance for infilled RC frames due to the local collapse of infill walls. This shift in modal properties means that an IM anchored to the initial, period of the undamaged frame can be rather inefficient when assessing non-linear behaviour. Past work by O’Reilly and Sullivan (2018b) has noted this particular feature; depending on the level of damage sustained by the infill panels, the efficiency of $Sa(T_1)$ was heavily influenced in what was termed the *cliff effect* (Fig. 6). This resulted because, for a set of records all scaled to the same value of $Sa(T_1)$, some ground motions caused a local infill collapse and pushed the response past the peak capacity of the infilled frame, responding in subsequent cycles with the blue reloading line, leading to large structural demands shown via the band of red points in Fig. 6. Other ground motions did not manage to push past the peak and remained in the range with relatively low demand prior to local infill collapse, indicated via the band of green points in Fig. 6. This differentiation between ground motions that caused bands of both high and low demands at the same intensity suggested that other factors were coming into play in such scenarios. It also meant that the $\beta_{EDPIIML}$ observed when using $Sa(T_1)$ as an IM for infilled RC frames was rather large, as illustrated via the demand-intensity curve shown in the right of Fig. 6. This was seen in Fig. 5 for both a 3 and 9 storey case study structure. Of note for the 9 storey structure in Fig. 5 is how the *PGA* dispersion is slightly higher, which is a reflection of the loss of its predictive power, or efficiency, for taller structures with longer vibration periods. Comparing this large dispersion in infilled RC frames when using $Sa(T_1)$ as the IM to the relatively lower dispersion for more conventional structures without infills, it is clear that there is room for improvement in terms of efficient response prediction.

O’Reilly and Sullivan (2018b) identified the spectral shape of the ground motions to be a potential reason for this segregation in demand. Records with a ‘valley’ shape tended to have higher demands than others with a ‘peaked’ shape (Baker and Cornell 2006). That study also utilised ground motion records as part of IDA which were not selected to match

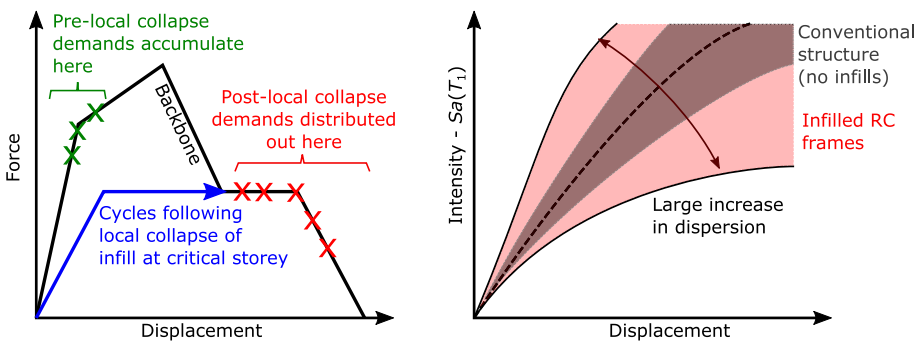


Fig. 6 Illustration of the cliff effect (O’Reilly and Sullivan 2018b) in infilled RC frames, whereby two bands of response at low and high demands for a given ground motion set giving an overall increased dispersion for $Sa(T_1)$ compared to conventional systems

a specific site hazard, meaning that better matching of spectral values across all periods to site hazard via a CS may reduce this effect. Further analysis by O'Reilly et al. (2018a) briefly addressed this through careful selection and scaling of ground motion records and noted this same trend. That study also trialled the potential use of *AvgSa* given the pertinence of period elongation in infilled RC frame dynamic response and noted a better characterisation of the behaviour. Figure 4b reaffirms these initial observations, with the $\beta_{EDPIIML}$ remaining relatively stable for *AvgSa*. Figure 5 further illustrates this with $\beta_{EDPIIML}$ tending to remain reasonably low across all intensity levels. *AvgSa* is seen to not be as efficient in the lower return periods corresponding to elastic response, but it remained a good overall performer for all return periods. Therefore, these observations from Figs. 4 and 5 suggest that when conducting intensity-based analyses of non-ductile infilled RC frames, such as those required by building codes for given return periods of shaking, the choice of IM used to select ground motions and conduct analysis can have a notable effect on the results obtained. The least efficient IMs (i.e. high $\beta_{EDPIIML}$), such as *PGA* or *Sa(T₁)* at higher return periods, will exhibit higher $\beta_{EDPIIML}$ and possibly require many more ground motion records to sufficiently characterise the response, whereas others such as *AvgSa* may be more computationally efficient. Other factors play a part in this discussion and will be addressed in later sections.

6.2 Fragility functions

While the response at discrete return periods is of interest in certain types of analysis and structural verifications, a more probabilistic description of structural response is of more direct interest in risk assessment. As stated previously, three limit states were considered in this study to evaluate the response of the infilled RC frames. A lognormal distribution with median, $\eta_{IML|EDP}$, and dispersion, $\beta_{IML|EDP}$ was fitted where the random variable under examination is now the intensity level required to exceed a given EDP level. For MSA, the fraction of ground motions causing a θ_{max} limit state exceedance at each T_R examined is shown via several dot markers in Fig. 7. With these fractions of exceedances known for a set of IMLs, the discrete distribution of IML for a given EDP limit state was established. The continuous lognormal fragility functions were fitted using these discrete fractions of EDP exceedances at each IML using the maximum likelihood method. When selecting the T_R range for which to conduct MSA, care was taken to ensure that an adequate number of exceedances were observed such that the whole range of response was characterised and fragility functions could be fitted. Each fragility function was tested like before for each structure, IM, and θ_{max} threshold value evaluated, with a lognormal distribution deemed suitable in each case. Figure 7 shows these fragility functions for the same case study structure examined previously.

While not of direct relevance to the current discussion, Fig. 7 also compares the fragility functions derived for the same 3 limit states using IDA results (to be discussed later) with the additional set of ground motions selected in Sect. 4. A hunt and trace algorithm (Vamvatsikos and Cornell 2004) was employed to allow the response right up to collapse to be characterised, so that the intensity resulting in collapse would be known with a degree of accuracy for each record. This differs from MSA where the number of collapses per intensity is known, but not the minimum intensity any one ground motion record would have needed to be scaled to result in structural collapse.

In Fig. 7, the MSA curves are taken as the reference set, considering the record selection applied at each hazard level used to derive them. For the most part, a general agreement

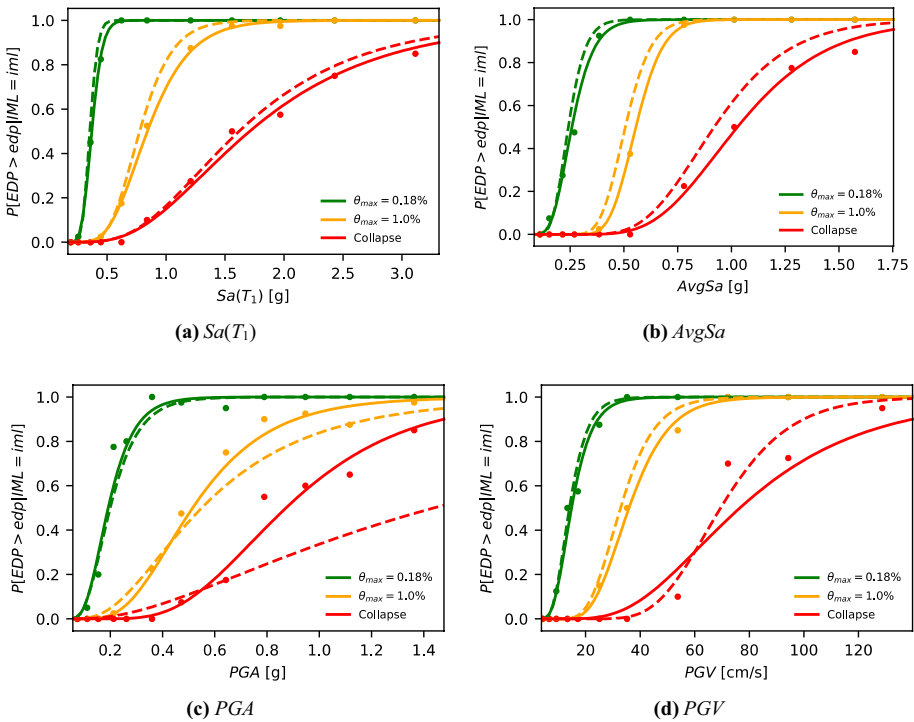


Fig. 7 Fragility functions for the 3 storey structure with weak infills (RC-WI-3) for the 4 IMs investigated. Note: each plot shows the MSA-based (solid line) fragility functions and the exceedance probabilities they were fitted to (dots) alongside the IDA-based fragility curves (dashed lines)

between the two sets is observed and was seen among all structures examined. All IMs were seen to match well between the two methods for $\theta_{max}=0.18\%$. This is an expected result, especially for $Sa(T_1)$, since the structures are still responding in the elastic range. It is with increasing damage to the infilled RC frames that the curves are seen to deviate for some cases. For the different case study structures, $Sa(T_1)$ and $AvgSa$ -based fragility functions tended to be reasonably well-matched for IDA and MSA and the sets presented in Fig. 7 are represented of all structures examined. For PGA and PGV , however, the results tended to be a bit more volatile with some cases, such as Fig. 7 for $\theta_{max}=1.0\%$, showing a fair agreement, whereas the collapse limit state showed a larger discrepancy. Of note is the discrepancy between the IDA-based and MSA-based fragility curves at collapse when using PGA and PGV . These are significantly different and may be attributed to the lack of sufficiency with respect to scaling factors used in IDA, which will be discussed in Sect. 7; it will be seen how the results obtained when using PGA and PGV were influenced by the large scaling factors applied to these records needed to induce collapse, whereas $Sa(T_1)$ and $AvgSa$ were not.

Another notable aspect in Fig. 7 is the relative magnitude of $\beta_{IM|IEDP}$ between the fragility curve IMs and limit states. This is indicative of the level of uncertainty and the general efficiency of the IMs in characterising the limit state exceedance. Figure 8 shows the mean $\beta_{IM|IEDP}$ of all case study structures for each limit state threshold. As with Fig. 7, it shows how PGA and PGV tended to have the highest $\beta_{IM|IEDP}$ across all limit states, suggesting

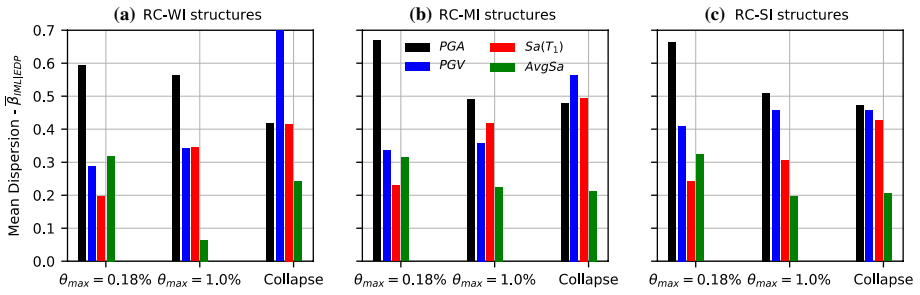


Fig. 8 Mean dispersion across all structure heights, $\bar{\beta}_{IM|IEDP}$, of the MSA-based fragility functions for each IM, masonry infill typology and limit state threshold examined

that they are relatively inefficient predictors of structural response for infilled RC frames. $Sa(T_1)$ was seen to start with the lowest mean $\beta_{IM|IEDP}$ for all IMs examined, indicating its high predictive power, but gradually lost its efficiency for more severe limit states. As anticipated, $AvgSa$ was seen to provide the most favourable solution in terms of IM efficiency, as it exhibited reasonably low $\beta_{IM|IEDP}$ at the onset of damage and maintained a similar level of predictability across all limit states. This resonates with the previous discussion, whereby the MSA results and fragility functions derived for $AvgSa$ indicated it to be a much more stable predictor of structural response to be used in future analysis and not exhibiting sensitivity to large jumps in dispersion with increased limit state, as in the case of $Sa(T_1)$.

7 Sufficiency

As discussed previously, one of the desired properties of an IM is sufficiency, meaning the structural response conditional to various IM levels ought to be independent of other rupture characteristics that produced each ground motion. Given that this study focusses on the efficiency and potential bias of different IMs for assessing infilled RC frames, it was necessary to first check their sufficiency to ensure that these aspects were not influential in the analysis results obtained.

Rupture characteristics such as moment magnitude, M , and Joyner-Boore distance, R_{jb} , are typically checked, along with the level of scaling, SF , applied to the record. These were checked here to evaluate the results presented in the previous section for different IMs. The sensitivity of both the non-collapse and collapse cases was examined and is discussed below. The collapse cases were checked via the IML required to induce collapse found via IDA and the non-collapse cases were checked by analysing the EDP values at each return period intensity analysed. The sufficiency of the results can be checked by examining their statistical significance with respect to different rupture characteristics, which is the approach followed herein, although recent studies analysing relevant sufficiency using information theory (Ebrahimian and Jalayer 2020; Jalayer et al. 2012; Du and Padgett 2020; Ebrahimian et al. 2015) could also be considered. This definition of relative sufficiency proposed by Jalayer et al. (2012), which differs to the metric of the same name utilised by Dávalos and Miranda (2019), uses the average difference between the information

gained about the EDP given two IMs compared to that gained given just one IM and has been utilised in several past studies (Minas and Galasso 2019; Song et al. 2020).

7.1 Non-collapse cases

To examine the sufficiency of the non-collapse cases, the records not resulting in collapse during MSA were utilised. Evaluation of the sufficiency was done by examining the θ_{\max} residuals, ϵ_θ , for each IM, defined for each ground motion i as:

$$\epsilon_{\theta,i|IML} = \frac{\theta_{\max,i|IML}}{\hat{\theta}_{\max|IML}} = \frac{\theta_{\max,i|IML}}{\exp\left(\frac{1}{n} \sum_{i=1}^n \ln(\theta_{\max,i|IML})\right)} \tag{1}$$

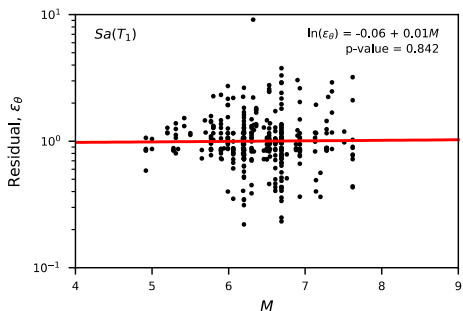
where n is the number of ground motions not causing collapse at a given IML. This residual describes the ratio of an observed response with respect to the median response value for an IM at that IML. It means that ground motions with high residuals reported a larger than usual response in the structure at that IML. To classify any of the investigated IMs' MSA results as sufficient for non-collapsing cases, it is typical (e.g. Luco and Bazzurro 2007) to look for a trend between these residuals and rupture parameters or scaling factor. This way, any dependence in results with respect to the median response becomes apparent. The functional form utilised in these tests was:

$$\ln(\epsilon_\theta) = \beta_{0,\theta} + \beta_{1,\theta}rup \tag{2}$$

where rup denotes any rupture parameter associated with the records selected. This relationship assumes that there is a linear relationship between the logarithm of the residuals and the rupture parameter. Figure 9 illustrates the type of data obtained and plotted in red is the trendline fitted via least square regression. Visual inspection of the fitted trendline suggests that there is very little relation between ϵ_θ and M . This is seen from the relatively horizontal nature of the trend line, whose coefficient was $\beta_{1,0}=0.01$, indicating little dependence.

To demonstrate that the results obtained are independent of rup , statistically significance tests were employed. To do this, the test hypothesis that there is no relationship between the residuals and the rup parameter (i.e. $\beta_{1,0}=0$) is set. By examining the actual data, like those shown in Fig. 9, the p value of the observed $\beta_{1,0}$ parameter can be computed and evaluated. The p value indicates the degree to which the observed data conform to the pattern predicted by the test hypothesis and the underlying statistical model (Greenland

Fig. 9 Illustration of the observed trend between non-collapse case residuals and moment magnitude for the case study structure RC-MI-2 analysed with ground motions selected and scaled for $Sa(T_1)$



et al. 2016). Therefore, a very low p value would indicate that the data are not very close to what the statistical model predicted they should be (i.e. there is likely some dependence on the rup parameter), whereas a large p value would indicate that the data are close to the model prediction (i.e. no relationship between the residuals and the rup parameter). A significance threshold of 5% is typically adopted and was used here. As shown in Fig. 9, the p value observed was 84.2%, well above the threshold of 5%, implying that the observed data is close to the test hypothesis prediction (i.e. no relationship) and the results deemed independent of M , as already deduced by visual inspection.

To investigate the sufficiency of each IM for each case study structure, their p values were computed and summarised for M and R_{jb} . While technically not a rupture parameter per se, SF was also checked to ensure that the results were not influenced by the scaling of the ground motions during record selection, as past studies (Luco and Bazzurro 2007) have noted. Figure 10 plots the cumulative distribution of all p -values for the structures analysed. That is, the p values computed for each case study structure listed in Table 1 were collected and plotted cumulatively to illustrate and summarise in a concise manner the general trend in statistical test results for all structures examined here. Past studies like Sousa et al. (2016) have also employed similar plots to illustrate general trends in statistical test results. It is important to note that these statistical test results are not taken as definitive proof of dependence (or independence), but rather used as an indicator to understand where dependencies may lie and be examined further in later sections.

For the vast majority of structures analysed, the residuals of the non-collapse case MSA results (indicated by the solid lines) obtained for different IMs were not influenced by M or R_{jb} , with just one or two cases exhibiting p -values lower than the threshold value for each IM. For what concerns SF , Fig. 10 indicates that the non-collapse cases could be assumed

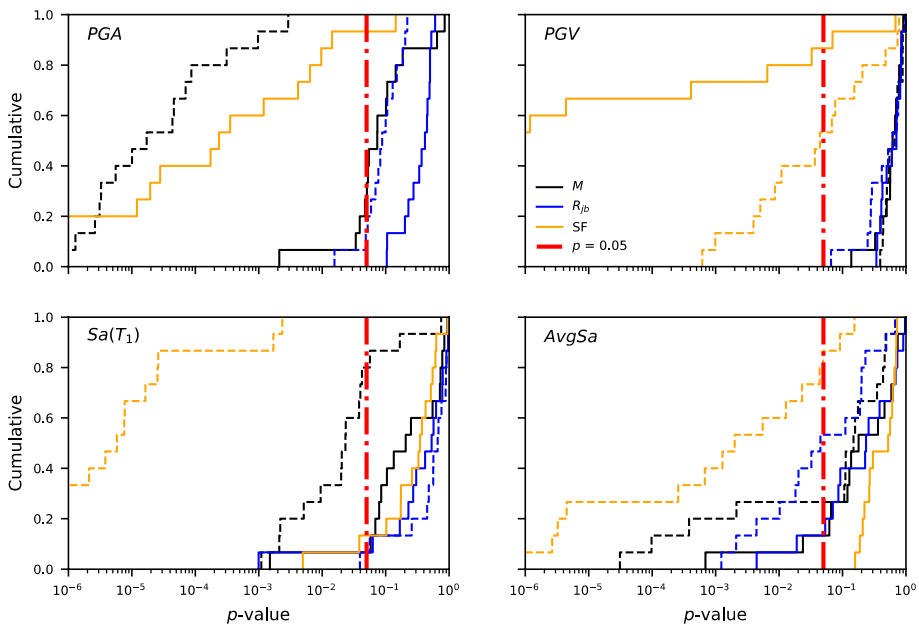


Fig. 10 Cumulative distribution of p -values observed for each case study structure, including those observed for the non-collapse cases from MSA (solid lines) and those observed for the collapse cases via IDA (dashed lines), for each IM and ground motion parameter investigated

independent of the SF used for $Sa(T_1)$ and $AvgSa$. It is worth noting that recent research by Ebrahimiyan and Jalayer (2020) has noted that when heavily scaled records are used, the differences in sufficiency (or lack thereof) between $Sa(T_1)$ and $AvgSa$ tends to become more accentuated. However, given both IMs are observed to be sufficient for all MSA analyses here, and the fact that $AvgSa$ will generally require lower scaling factors in record selection than $Sa(T_1)$ (Kohrangi et al. 2017), this issue is not deemed problematic herein. For PGA and PGV , it can be seen that almost all of the case studies exhibited p -values lower than the threshold, meaning that there is likely a dependence on the SF .

7.2 Collapse cases

To examine the sufficiency of the collapse results obtained for each case study structure, a similar process was followed. As mentioned previously, IDA was utilised to characterise the collapse intensity using 60 ground motions. MSA collapse cases were not utilised because of the format of the results. For a given IML in MSA, some collapses may be observed. However, the precise intensity at which a particular scaled ground motion record causes structural collapse is not known since the results are reported in a binary ‘collapse’ or ‘no collapse’ format for a given IML. The actual collapse intensity value for a particular ground motion may have been a little less than the IML for which the results were reported. Since it is these collapse causing intensities that are to be examined, IDA was employed following a hunt and fill algorithm to more accurately determine the collapse intensity for each ground motion. As before, the residuals were examined to determine whether there was any dependence of the collapse intensities, s (as opposed to structural demand θ_{max} in the non-collapse cases) on the ground motion rupture parameters. These intensity-based residuals, ϵ_s , were defined as follows for a given ground motion i causing collapse in a case study structure:

$$\epsilon_{s,i} = \frac{s_i}{\hat{s}} = \frac{s_i}{\exp\left(\frac{1}{n} \sum_{i=1}^n \ln(s_i)\right)} \tag{3}$$

where n is the number of ground motions used in IDA, which was 60. Note that these residuals are different in nature to those defined by Eq. (1), with lower values of ϵ_s and higher values of ϵ_θ representing more aggressive ground motion records. Again, the relative trends between the collapse residuals and the ground motion parameters examined previously were scrutinised. As before, the p values of $\beta_{1,s}$ from the following expression were examined:

$$\ln(\epsilon_s) = \beta_{0,s} + \beta_{1,s}rup \tag{4}$$

The results are shown via the dashed lines in Fig. 10. Similar to before, the cumulative values for all case study structures vary depending on the IM and the rupture parameter being examined. For M , the collapse results quantified using PGA showed a dependence, with some cases for $Sa(T_1)$ and $AvgSa$ falling below the significance threshold (i.e. dependent) whereas the PGV results show no issues. For R_{jb} , Fig. 10 suggests no relationship for all IMs (i.e. sufficient). For SF , a statistical dependence of all IMs (PGA values are much lower than the axis limits and are not visible). This is problematic as it suggests that all IMs are influenced by the level of scaling applied to them when conducting IDA, although comparisons of the fragility functions derived via both MSA and IDA in Sect. 6.2 indicated

that this dependence may not be significant. Overall, these results suggest that the collapse capacity quantified using each IM, with the exception of *PGA*, is independent of ground motion rupture parameters. However, each IM was seen to be influenced by the level of scaling applied to it in IDA.

8 Bias

Section 7 discussed the sufficiency of structural response with respect to rupture parameters and scaling factor, whereas Sect. 6 examined the relative efficiency of each IM. They showed how of the four IMs examined here in the context of assessing infilled RC frames, *PGA* and *PGV* were generally the least efficient in terms of response prediction and were noted to be influenced by the scaling factor applied to the records. $Sa(T_1)$ and *AvgSa* showed no such influence when following a MSA approach: $Sa(T_1)$ was also observed to be the most efficient at initial damage limit states but lost its efficiency towards collapse, whereas *AvgSa* remained a reasonably good predictor of response. Some dispersion is generally expected for all IMs due to the inherent randomness of ground motions and the difficulty of accurately characterising the non-linear response of a multi-modal structure via a simple IM, amongst other sources of uncertainty: it is noted that structural response uncertainty in this study only deals with record-to-record variability. However, there may be instances where a notable dispersion may not necessarily be due solely to the natural, or aleatory, uncertainty in characterising the response, but rather from a single pertinent ground motion characteristic biasing the response. As mentioned previously, a simple example of bias is the study by Chandramohan et al. (2016) regarding the impact of ground motion duration on collapse capacity: long duration records resulted in lower collapse capacity than spectrally equivalent short duration records; had record duration not been considered and results from all records used collectively to develop fragility curves, a large scatter would have resulted in the collapse intensities due to the hidden bias of the long duration records.

Bradley (2012b) discussed such bias within the context of ground motion record selection. He noted how for some scenarios, the results obtained using ground motions selected and scaled to a single conditioning IM termed IM_j (e.g. $Sa(T_1)$) could also depend on, or be biased by, another IM denoted IM_i (e.g. ground motion duration). What was important to note was this is not necessarily a problem if both IM_j and IM_i are selected to be consistent with the site hazard. Hazard consistency is taken here to mean that the respective rates of exceedance of the ground motions' IM_j and IM_i are consistent with, or match, the site hazard curves obtained from PSHA. This culminated in the development of the generalised conditional intensity measure (GCIM) approach (Bradley 2010) to deal with situations where more than one IM is pertinent, leading to a more robust and comprehensive ground motion record selection and subsequent risk assessment. To investigate whether the efficiency of the IMs examined here (i.e. IM_j) was influenced by other ground motion parameters (i.e. IM_i), it was necessary to see whether the results exhibited any notable dependence on these IM_i parameters. Should the results exhibit no bias, then IMs can be evaluated based on the results presented in Sects. 6 and 7. But should a bias be found, then it would shed further light on the efficiencies observed previously. This section therefore examines the results of the infilled RC frames characterised via different IMs with respect to other ground motion properties to shed further light on the results obtained so far.

8.1 Ground motion IM_j parameters examined

To investigate potential bias in the results presented previously, several other IM_j parameters were identified. These were: PGA ; PGV ; 5–75% significant duration, $D_{s,5-75}$, defined by Trifunac and Brady (1975); incremental velocity, IV , defined by Bertero et al. (1978); and filtered incremental velocity, $FIV3$, defined by Dávalos and Miranda (2019). Significant duration defined between the cumulative percentages 5–75%, $D_{s,5-75}$, was noted by Chandramohan et al. (2016) to have an impact on the collapse response of degrading systems and to be the best among the different quantifiers of duration examined. Velocity-based IMs have been considered for many years, with some early work by Bertero et al. (1978) noting the damaging impact of velocity pulses during the 1971 San Fernando earthquake. This led them to propose IV , defined as the maximum area beneath individual acceleration pulses. Studies by Jayaram et al. (2010) showed that among different IMs considered, IV was the best predictor of displacement-based demands for infilled RC frames. Recent work by Dávalos and Miranda (2019) has improved on the definition of IV through the development of $FIV3$. The original shortcomings of IV surrounding its period independence, its local interruption of velocity pulses through high frequency-induced zero-crossings, and neglect of cumulative pulses were directly addressed. Dávalos and Miranda (2019) have shown $FIV3$ to be a much improved predictor of structural collapse compared to IV and other IMs.

8.2 Statistical testing

8.2.1 Non-collapse cases

Like sufficiency discussed in Sect. 7.1, the non-collapse results were also examined for independence to other ground motion characteristics. That is, the conditioning intensity measure, IM_j (Sect. 3), was assumed to be capable of fully describing the non-collapse response. The residuals defined in Eq. (1) were therefore checked for statistical significance assuming the same functional form of Eq. (2), where rup was replaced by the individual IM_j parameters listed in Sect. 8.1. In particular, the relationship between the natural logarithm of the residual ϵ_0 was compared with $D_{s,5-75}$ and the natural logarithm of PGA , PGV , IV and $FIV3$. The p -values were computed for each structure and the cumulative values for all case study structures are plotted in Fig. 11. They are then compared with the threshold significance of $p = 5\%$.

As expected, the $IM_j = PGA$ and $IM_j = PGV$ results are seen in Fig. 11 to be completely dependent on the parameters $IM_j = PGA$ and $IM_j = PGV$, respectively, which should be an obvious conclusion. Examining for $IM_j = PGA$, the results possessed some degree of dependence on almost all IM_j parameters evaluated, with all except $D_{s,5-75}$ exhibiting $p < 5\%$. For $IM_j = PGV$, dependence was observed for each IM_j parameter with the exception of IV . When using $IM_j = Sa(T_1)$, the results were influenced by each of the velocity-based IM_j parameters (i.e. PGV , IV and $FIV3$) whilst being somewhat independent of PGA and $D_{s,5-75}$. Lastly, when $IM_j = AvgSa$, the non-collapse cases are observed to be independent of velocity-based properties of the ground motions, contrary to $Sa(T_1)$, although some significance of PGA and $D_{s,5-75}$ was noted.

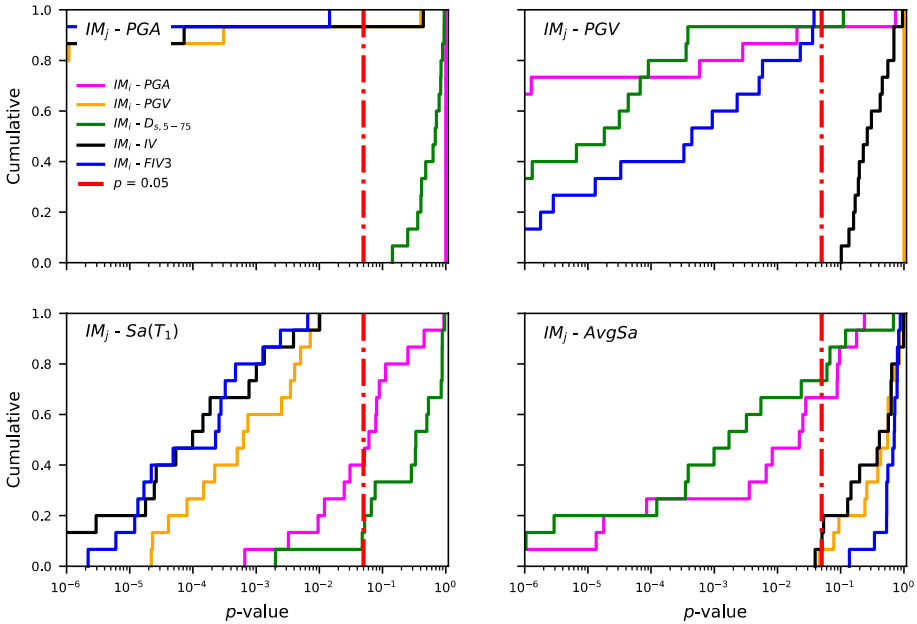
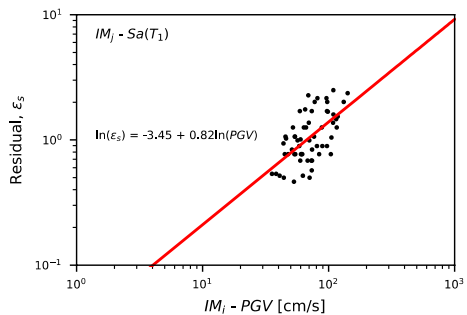


Fig. 11 Cumulative distribution of p -values observed for non-collapse cases from MSA of each case study structure, where each subplot shows each conditioning IM_j for each ground motion IM_i investigated

8.2.2 Collapse cases

For the collapse cases, the same test to show independence from IM_i parameters could not be done. Contrary to non-collapse cases, where the residuals ϵ_0 were examined, collapse cases were examined using collapse intensity residuals, ϵ_{cs} , meaning that an intensity-based quantity was being compared with another intensity-based quantity. Therefore, some degree of dependence should be expected when using the functional form of Eq. (4) with rup replaced by IM_i . Using the test hypothesis of $\beta_{1,s} = 0$ would not yield much insight because if a record causing collapse had a relatively high $Sa(T_1)$ value, then the PGV of the same record would also be expected to be high (i.e. $\beta_{1,s} > 0$) due to the known correlation (Bradley 2012a) between $Sa(T_1)$ and PGV , as shown in Fig. 12, for example. Instead, a more simplified approach was followed here where a dependence was assumed (i.e. $\beta_{1,s} \neq 0$) and the magnitude of it for the different IM_i and IM_j pairs was compared relatively.

Fig. 12 Illustration of the observed trend between collapse residuals, ϵ_s , when $IM_j = Sa(T_1)$ and $IM_i = PGV$ for the RC-6-MI case study structure, where the correlation (i.e. $\beta_{1,s} > 0$) is evident



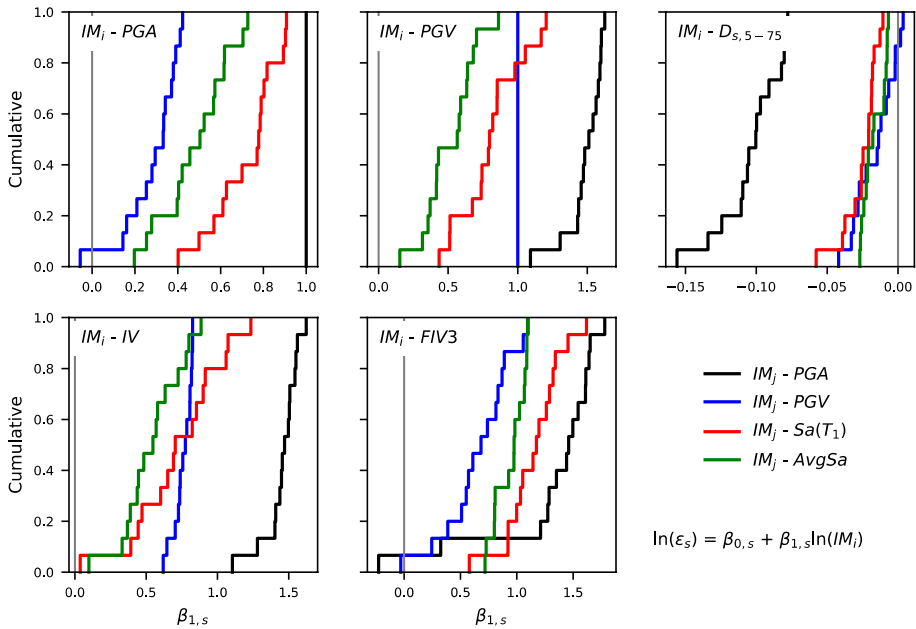


Fig. 13 Cumulative distribution of the $\beta_{1,s}$ values observed for collapse cases from IDA of each case study structure, where each subplot shows each ground motion IM_i investigated for each conditioning IM_j

Therefore, for each IM_j examined (Sect. 3), the collapsing intensity residuals ϵ_s were computed using Eq. (3). Equation (4) was then used, with *rup* being replaced by each of the IM_i parameters listed in Sect. 8.1, and the trend was fitted using least squares regression. The relative magnitude of $\beta_{1,s}$ was then examined, with the cumulative values shown in Fig. 13 for all case study structures.

Examining the relative influences shown in Fig. 13, it is noted how for $IM_j = PGA$, the collapse residuals are strongly influenced by all other IM_i parameters, much more than the other IM_j and especially for duration. When $IM_j = PGV$, these collapse results are generally those least influenced by other IM_i parameters, indicating more favourable characteristics for what concerns potential bias when evaluating the collapse of infilled RC frames. Cases of $IM_j = Sa(T_1)$ were not too different to PGA in that they were influenced by other IM_i parameters. Lastly, it can be seen that $IM_j = AvgSa$ was similar to PGV as it had a comparatively low influence with respect the other IM_i parameters.

8.3 Further examination

From previous sections, it was seen how the results for $IM_j = PGA$ and $IM_j = PGV$ had a statistically significant dependence for several other IM parameters. Also notable was the consistent trend of $IM_j = Sa(T_1)$ results to the velocity-based IM_i parameters illustrated in Fig. 11, whereas the *AvgSa* results were shown to be relatively independent in comparison.

These results are examined in further detail here to see if this dependence on the velocity characteristics of the $IM_j = Sa(T_1)$ results can be illustrated in structural engineering quantities instead of statistical terms, as has been done up to now. To do this, the case study structure RC-WI-3 was again considered. Its MSA results were plotted in Fig. 4 and the

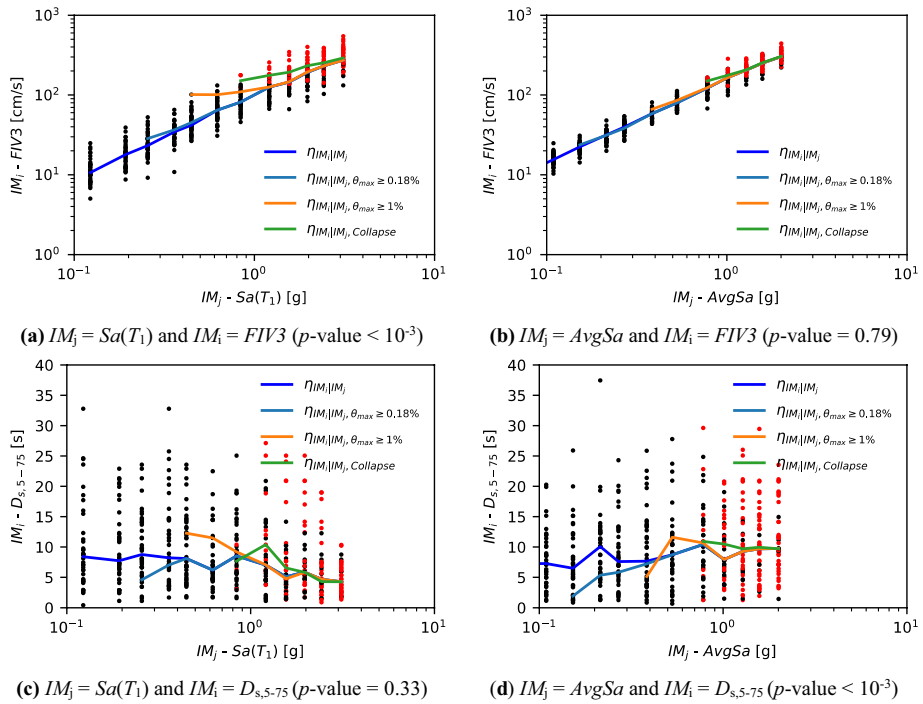


Fig. 14 Comparison of the median IM_i values for a given IM_j for the case study structure RC-WI-3, illustrating the potential bias in response at different limit states as a result of IM_i . Note Points plotted in red represent collapsing cases and p -values are reported for the non-collapse cases in the parentheses from Fig. 11

$\beta_{EDP_{IIML}}$ dispersions at each return period were shown in Fig. 5. For each of these MSA stripes with conditioning IM_j shown on the horizontal axis in Fig. 14, the corresponding IM_i values of each ground motion were plotted via markers on the vertical axis. This distribution of IM_i/IM_j at each intensity is what indirectly results when selecting ground motions conditioned on IM_j alone. This is the distribution for several types of IM_i that the GCIM intends to check and ensure hazard consistency for when selecting records (i.e. that the IM_i/IM_j of the selected ground motions matches the site hazard). This was noted by Bradley (2012b, 2010) to be an important consideration when IM_i is observed to be a biasing parameter on the structural response, but could be left unconditioned for IMs that do not show a biasing influence on the response.

In order to examine bias due to these IM_i , the results were segregated based on the EDP threshold value exceedances of each response point, which was θ_{max} in this case. First, the median values of IM_i at each MSA stripe level IM_j , $\eta_{IM_i|IM_j}$, were computed and plotted as the median trend for that IM_i . Then, for the three limit states described previously in Sect. 5, response analysis points exceeding these EDP thresholds denoted $x\%$ were extracted and their median value for each given MSA stripe at IM_j was computed as $\eta_{IM_i|IM_j, \theta_{max} \geq x\%}$. This then gave what will be termed the uncensored (i.e. $\eta_{IM_i|IM_j}$) and censored (i.e. $\eta_{IM_i|IM_j, \theta_{max} \geq x\%}$) median values of IM_i for a given EDP limit state and value of IM_j . These are shown in Fig. 14 for the case study structure RC-WI-3 when $IM_i = FIV3$ and $D_{s,5-75}$ for $IM_j = Sa(T_1)$ and $AvgSa$. This comparison illustrates the influence of IM_i on the

structural response in a relatively simple manner. Should there be no biasing impact of IM_i on the response analysis results, the censored and uncensored medians will be closely aligned (i.e. $\eta_{IM_i|IM_j} \approx \eta_{IM_i|IM_j, \theta_{\max} \geq x\%}$). A biasing IM_i on the other hand, will show a deviation between the two (i.e. $\eta_{IM_i|IM_j} \neq \eta_{IM_i|IM_j, \theta_{\max} \geq x\%}$).

The observations from Sect. 8.2.1 are recalled, where results for $IM_j = Sa(T_1)$ were seen to be dependent on the velocity-based characteristics of the ground motions, whereas the $IM_j = AvgSa$ cases did not. This can be more clearly seen in Fig. 14a, b via the relative trends of the uncensored and censored medians with respect to their $IM_i = FIV3$ values. For $IM_j = Sa(T_1)$ in Fig. 14a, it can be seen that the two lines match for the limit state of $\theta_{\max} = 0.18\%$ meaning that its exceedance was likely not caused by a ground motion with a particularly high $FIV3$. For $\theta_{\max} = 1.0\%$ and collapse, a difference between the censored and uncensored trends can be seen, showing that ground motion records with higher $FIV3$ tended to cause the limit state to be exceeded. This is evidence of the biasing effect of the velocity-based IMs such as $FIV3$ on the $IM_j = Sa(T_1)$ results. On the other hand for the cases of $IM_j = AvgSa$, it can be seen that these results did not present such an impact given that the censored and uncensored trends align well. This illustrates them to be relatively independent of such bias, as was noted in Sect. 8.2.1. The p -values reported in each sub-caption of Fig. 14 correspond to this specific case study structure's non-collapse cases p -values, which were described in Sect. 8.2.1 and summarised for all structures in Fig. 11.

Figure 14c, d show the same comparison with respect to $IM_i = D_{s,5-75}$, where no clear trend or biasing effect of the duration on results for $IM_j = AvgSa$ with respect to $IM_j = Sa(T_1)$ appears evident. This was confirmed through inspection of similar results for other case study structures. It was observed, that instances of $p < 0.05$ for both $IM_j = AvgSa$ and $IM_j = Sa(T_1)$ resulted for datasets with a relatively narrow range of $IM_i = D_{s,5-75}$ values hence caution in interpreting these results is advised. Further studies with ground motions of a wider duration range should be utilised to further investigate this as it may appear contrary to past research on the impacts of ground motion duration on structural response.

8.4 Remarks

In light of the above observations, some final comments are given. From past work and also that shown here, it is clear that using $IM_j = Sa(T_1)$ as an IM to characterise the behaviour of infilled RC frames poses some issues. This was previously observed via the large dispersion in dynamic response discussed in Sect. 6 and shown in Figs. 5 and 8. This was initially attributed to the spectral shape of the records and the period elongation of the systems (O'Reilly and Sullivan 2018b), but further analysis in Sect. 8 showed this to be closely related to velocity-based characteristics of the ground motion records, which have been known to be influential on the collapse of structures, but not been clearly demonstrated for this structural typologies in past research. What was very curious and promising to note was that the $IM_j = AvgSa$ results did not seem to have this same pitfall as the $IM_j = Sa(T_1)$ results, since no notable jump in dispersion or significant bias in the response due to velocity-based properties was noted. The immediate question to ask is: why not? After all, $AvgSa$ is just a geometric mean of $Sa(T)$ values located around, or close to, T_1 . One possibility is that the averaging effect of $AvgSa$ helps minimise the influence of pulses for systems sensitive to them, as Eads et al. (2015) noted. A detailed study (Eads and Miranda 2013) found that a response spectrum, or more specifically its spectral shape, could be viewed as a reflection of a few critical velocity pulses in a record. Hence, $AvgSa$'s incorporation of

many spectral acceleration values, and consequently the spectral shape, could be indirectly accounting for these damaging velocity pulse characteristics of the ground motions. This would suggest that the analysis results are less likely to be biased by such damaging pulses, as has been observed here.

In favour of $IM_j = Sa(T_1)$, however, are the fact that it has been simpler to obtain its hazard curve needed to compute risk than it has been for $IM_j = AvgSa$ until recently (i.e. $Sa(T_1)$'s hazard is more computable than $AvgSa$). While most hazard tools are well-equipped for computing hazard for $IM_j = Sa(T_1)$, recent updates to the OpenQuake hazard engine now allow the computation of $IM_j = AvgSa$ with ease making equally obtainable. Also, using $IM_j = Sa(T_1)$ has the added benefit of a physical meaning of the IM's definition with respect to the structure's initial dynamic properties. Maintaining $IM_j = Sa(T_1)$ for these reasons is not a problem depending on the analysis objectives and methods employed. If the initial behaviour prior to local infill collapses is being examined then there should be no major problems, but if extensive damage and collapse are being analysed then further care is needed. With regards to risk, the relative uncertainty in the IM hazard curves is worth mentioning because if the uncertainty in the $IM_j = AvgSa$ hazard curve outweighs the gain in prediction capability with respect to $IM_j = Sa(T_1)$, the overall risk estimate would not be greatly improved. However, Kohrangi et al. (2017) have shown that the overall uncertainty is in fact reduced when $IM_j = AvgSa$ due to its increased predictability of the IM, which alleviates such a concern.

Another important point to note is that the ground motion records utilised here were selected to match the site hazard for a single IM_j , with other ground motion intensity parameters IM_i accepted for what they were without any extra effort to be hazard-consistent. Ideally, ground motions should be hazard-consistent for all IMs but in practice, this is only needed when the EDPs are sensitive to these other IM_i parameters (Bradley 2012b). This presents a very significant advantage of $IM_j = AvgSa$ over $IM_j = Sa(T_1)$ as an IM for the assessment of infilled RC frames. In short, many of the less desirable features or problems of $IM_j = Sa(T_1)$ can be overcome by simply switching to $IM_j = AvgSa$.

In light of these results, two possible solutions seem plausible for an appropriate seismic assessment of infilled RC frames: 1) using the classical conditional spectrum approach to selecting ground motions with $AvgSa$, as outlined by Kohrangi et al. (2017); or 2) using the GCIM (Bradley 2010) approach to record selection (Bradley 2012c) with $IM_j = Sa(T_1)$ but ensuring that the velocity-based characteristics (i.e. PGV , IV , $FIV3$) are hazard-consistent. Additional considerations can be made (e.g. duration effects) but what is clear is that there is a strong case for not using $Sa(T_1)$ by itself for these structural typologies.

9 Summary and conclusions

This article has examined the seismic assessment of non-ductile infilled reinforced concrete (RC) frames utilising different intensity measures (IMs). It examined the response of several case study structures at a site in Italy to characterise the seismic response via multiple stripe analysis (MSA), where ground motions were selected and scaled for numerous return periods, and incremental dynamic analysis (IDA) where a single set was scaled incrementally until the structure collapsed. The general response of the structures in terms of dispersion and efficiency was examined in relation to both intensity-based assessment along with risk-based fragility function development. The sufficiency of each IM with respect to ground motion rupture parameters was investigated and the potential bias introduced in

some IMs' characterisation of seismic response was also examined and highlighted. From the results of this study, the following points can be noted:

- For intensity-based assessment, examining the dispersion in demand at a given return period, *PGA* and *PGV* reported largest values, with $Sa(T_1)$ showing low dispersion initially but quickly climbing for higher ones, and *AvgSa* tended to have a moderately low level of dispersion across all intensities suggesting it may be a preferred candidate for intensity-based verifications required by building codes when analysing these typologies;
- For demand-based assessment, examining the dispersion in intensities required to exceed a given drift demand, *PGA* and *PGV* were again seen to have relatively high dispersions, $Sa(T_1)$ showed the same initial high efficiency but gradually became highly disperse, while *AvgSa* exhibited a relatively moderate dispersion throughout. This suggests that when building intensity-based fragility functions for buildings, as is done in regional assessment, the consistent and relatively low dispersion across limit states seen with *AvgSa* would make these fragility functions more accurate;
- Briefly comparing the derivation of fragility functions using both multiple stripe analysis (MSA) and incremental dynamic analysis (IDA), it was seen how when using *PGA* and *PGV* that some discrepancies arose between the two sets, whereas for $Sa(T_1)$ and *AvgSa* they tended to coincide quite well for the structures analysed;
- All IMs were generally observed to be sufficient, meaning that results were not dependent on ground motion rupture parameters like magnitude or distance. *PGA* and *PGV* were observed to be sensitive to the level of scaling applied to the ground motions when utilising MSA, whereas all IM results showed some dependence to scaling when utilising IDA;
- Examining the results for potential bias due to other ground motion IM parameters showed that when using *PGA* and *PGV*, the results tended to show a dependence on all other parameters investigated;
- Structural response when using $Sa(T_1)$ as the IM were shown to depend on the velocity-based parameters of the ground motion records used for the typologies examined. This supports previous findings regarding the large dispersion in response of infilled RC frames, which was further investigated here and attributed to the biasing effect of the velocity-based characteristics of ground motions used;
- Similar analysis of the structural response when using *AvgSa* as an IM showed no such dependence as in the case of $Sa(T_1)$, giving it a more consistent response prediction with reasonable dispersion and insensitivity to other ground motion parameters found to be problematic for the other IMs examined here.

Overall, this study has shown that classic IMs like *PGA* and *PGV* to possess a number of issues when used as part of intensity or risk-oriented assessments of non-ductile infilled RC frames. The pitfalls and reasons for undesirable high levels of dispersion when predicting structural response via $Sa(T_1)$ was scrutinised and found to possess several notable, although not insurmountable, snags. The relatively new addition to seismic risk assessment, *AvgSa*, was seen to indirectly dampen many of these issues without much extra effort. Hence, the choice in these situations remains whether to maintain and adjust the classic IM of $Sa(T_1)$ for non-ductile infilled RC frames or whether it would be better to utilise a more promising alternative in *AvgSa*.

Funding The work presented in this paper has been developed within the framework of the project “Dipartimenti di Eccellenza”, funded by the Italian Ministry of Education, University and Research at IUSS Pavia.

Declarations

Conflicts of interest The author declares to have no conflicts of or competing interests.

References

- Agudelo J, López R (2009) Fragility curves for infilled frames. Case study: structures of one and two levels in Puerto Rico. *Rev Int Desastres Nat Accid Infrastruct Civ* 9(1–2):163–186
- Akkar S, Sucuoğlu H, Yakut A (2005) Displacement-based fragility functions for low- and mid-rise ordinary concrete buildings. *Earthq Spectra* 21(4):901–927. <https://doi.org/10.1193/1.2084232>
- Baker JW (2011) Conditional mean spectrum: tool for ground-motion selection. *J Struct Eng* 137(3):322–331. [https://doi.org/10.1061/\(ASCE\)ST.1943-541X.0000215](https://doi.org/10.1061/(ASCE)ST.1943-541X.0000215)
- Baker JW, Jayaram N (2008) Correlation of spectral acceleration values from NGA ground motion models. *Earthq Spectra* 24(1):299–317. <https://doi.org/10.1193/1.2857544>
- Baker JW, Allin Cornell C (2006) Spectral shape, epsilon and record selection. *Earthq Eng Struct Dyn* 35(9):1077–1095. <https://doi.org/10.1002/eqe.571>
- Bertero VV, Mahin SA, Herrera RA (1978) Aseismic design implications of near-fault san fernando earthquake records. *Earthq Eng Struct Dyn* 6(1):31–42. <https://doi.org/10.1002/eqe.4290060105>
- Bojórquez E, Iervolino I (2011) Spectral shape proxies and nonlinear structural response. *Soil Dyn Earthq Eng* 31(7):996–1008. <https://doi.org/10.1016/j.soildyn.2011.03.006>
- Borzi B, Crowley H, Pinho R (2008) The influence of infill panels on vulnerability curves for RC buildings. In: 14th World conference on earthquake engineering (14WCEE), p 8
- Bradley BA (2010) A generalized conditional intensity measure approach and holistic ground-motion selection. *Earthq Eng Struct Dyn* 39(2):1321–1342. <https://doi.org/10.1002/eqe.995>
- Bradley BA (2012a) Empirical correlations between peak ground velocity and spectrum-based intensity measures. *Earthq Spectra* 28(1):17–35. <https://doi.org/10.1193/1.3675582>
- Bradley BA (2012b) The seismic demand hazard and importance of the conditioning intensity measure. *Earthq Eng Struct Dyn* 41(11):1417–1437. <https://doi.org/10.1002/eqe.2221>
- Bradley BA (2012c) A ground motion selection algorithm based on the generalized conditional intensity measure approach. *Soil Dyn Earthq Eng* 40(September):48–61. <https://doi.org/10.1016/j.soildyn.2012.04.007>
- Bradley BA, Dhakal RP, MacRae GA, Cubrinovski M (2009) Prediction of spatially distributed seismic demands in specific structures: ground motion and structural response. *Earthq Eng Struct Dyn*. <https://doi.org/10.1002/eqe.954>
- Carofilis W, Perrone D, O’Reilly GJ, Monteiro R, Filiatrault A (2020) Seismic retrofit of existing school buildings in Italy: performance evaluation and loss estimation. *Eng Struct* 225(December):111243. <https://doi.org/10.1016/j.engstruct.2020.111243>
- Chandramohan R, Baker JW, Deierlein GG (2016) Quantifying the influence of ground motion duration on structural collapse capacity using spectrally equivalent records. *Earthq Spectra* 32(2):927–950. <https://doi.org/10.1193/122813EQS298MR2>
- Cornell CA, Krawinkler H (2000) Progress and challenges in seismic performance assessment. *PEER Center News* 3(2):1–2
- Crisafulli FJ, Carr AJ, Park R (2000) Analytical modelling of infilled frame structures—a general review. *Bull N Z Soc Earthq Eng* 33(1):30–47
- Dávalos H, Miranda E (2019) Filtered incremental velocity: a novel approach in intensity measures for seismic collapse estimation. *Earthq Eng Struct Dyn* 48(12):1384–1405. <https://doi.org/10.1002/eqe.3205>
- Du A, Padgett JE (2020) Entropy-based intensity measure selection for site-specific probabilistic seismic risk assessment. *Earthq Eng Struct Dyn*. <https://doi.org/10.1002/eqe.3346>
- Eads L, Eduardo M (2013) Seismic collapse risk assessment of buildings: effects of intensity measure selection and computational approach. In: Blume Report No. 184. <http://purl.stanford.edu/cn733sv2623>
- Eads L, Miranda E, Lignos D (2016) Spectral shape metrics and structural collapse potential. *Earthq Eng Struct Dyn* 45(10):1643–1659. <https://doi.org/10.1002/eqe.2739>
- Eads L, Miranda E, Lignos DG (2015) Average spectral acceleration as an intensity measure for collapse risk assessment. *Earthq Eng Struct Dyn* 44(12):2057–2073. <https://doi.org/10.1002/eqe.2575>

- Ebrahimian H, Jalayer F (2020) Selection of seismic intensity measures for prescribed limit states using alternative nonlinear dynamic analysis methods. *Earthq Eng Struct Dyn*. <https://doi.org/10.1002/eqe.3393>
- Ebrahimian H, Jalayer F, Lucchini A, Mollaioli F, Manfredi G (2015) Preliminary ranking of alternative scalar and vector intensity measures of ground shaking. *Bull Earthq Eng* 13(10):2805–2840. <https://doi.org/10.1007/s10518-015-9755-9>
- Erberik MA (2008) Fragility-based assessment of typical mid-rise and low-rise RC buildings in Turkey. *Eng Struct* 30(5):1360–1374. <https://doi.org/10.1016/j.engstruct.2007.07.016>
- FEMA (2012) FEMA P-58-1: seismic performance assessment of buildings. Methodology, vol 1, Washington
- Del Gaudio C, De Martino G, Di Ludovico M, Manfredi G, Prota A, Ricci P, Verderame GM (2017) Empirical fragility curves from damage data on RC buildings after the 2009 L'Aquila earthquake. *Bull Earthq Eng* 15(4):1425–1450. <https://doi.org/10.1007/s10518-016-0026-1>
- Del Gaudio C, Di Ludovico M, Polese M, Manfredi G, Prota A, Ricci P, Verderame GM (2019a) Seismic fragility for Italian RC buildings based on damage data of the last 50 years. *Bull Earthq Eng*. <https://doi.org/10.1007/s10518-019-00762-6>
- Del Gaudio C, Risi MTD, Ricci P, Verderame GM (2019b) Empirical drift-fragility functions and loss estimation for Infills in reinforced concrete frames under seismic loading. *Bull Earthq Eng* 17(3):1285–1330. <https://doi.org/10.1007/s10518-018-0501-y>
- GEM (2019) The OpenQuake Engine User Instruction Manual. p 189. <https://doi.org/10.13117/GEM.OPENQUAKE.MAN.ENGINE.3.7.1>
- Giovenale P, Allin Cornell C, Esteva L (2004) Comparing the adequacy of alternative ground motion intensity measures for the estimation of structural responses. *Earthq Eng Struct Dyn* 33(8):951–979. <https://doi.org/10.1002/eqe.386>
- Glaister S, Pinho R (2003) Development of a simplified deformation-based method for seismic vulnerability assessment. *J Earthq Eng* 7(sup001):107–140. <https://doi.org/10.1080/13632460309350475>
- Greenland S, Senn SJ, Rothman KJ, Carlin JB, Poole C, Goodman SN, Altman DG (2016) Statistical tests, P values, confidence intervals, and power: a guide to misinterpretations. *Eur J Epidemiol* 31(4):337–350. <https://doi.org/10.1007/s10654-016-0149-3>
- Hak S, Morandi P, Magenes G, Sullivan TJ (2012) Damage control for clay masonry infills in the design of RC frame structures. *J Earthq Eng* 16(sup1):1–35. <https://doi.org/10.1080/13632469.2012.670575>
- Haselton CB, Baker JW (2006) Ground motion intensity measures for collapse capacity prediction: choice of optimal spectral period and effect of spectral shape. In: 8th US National Conference on Earthquake Engineering 2006, vol 15, pp 8830–8839
- HAZUS (2003) Multi-hazard loss estimation methodology—earthquake model. Washington.
- Jalayer F (2003) Direct probabilistic seismic analysis: implementing non-linear dynamic assessments. USA: PhD Thesis, Stanford University
- Jalayer F, Cornell CA (2009) Alternative non-linear demand estimation methods for probability-based seismic assessments. *Earthq Eng Struct Dyn* 38(8):951–972. <https://doi.org/10.1002/eqe.876>
- Jalayer F, Beck JL, Zareian F (2012) Analyzing the sufficiency of alternative scalar and vector intensity measures of ground shaking based on information theory. *J Eng Mech* 138(3):307–316. [https://doi.org/10.1061/\(ASCE\)EM.1943-7889.0000327](https://doi.org/10.1061/(ASCE)EM.1943-7889.0000327)
- Jayaram N, Bazzurro P, Mollaioli F, De Sortis A, Bruno S (2010) Prediction of structural response in reinforced concrete frames subjected to earthquake ground motions. In: 9th US National and 10th Canadian conference on earthquake engineering 2010, including papers from the 4th international Tsunami symposium, May 2014, vol 9, pp 7138–47
- Kappos AJ, Panagiotopoulos C, Panagopoulos G, El Papadopoulos (2003) Reinforced Concrete Buildings (Level 1 and Level 2 Analysis). In: WP4 Report RISK-UE
- Kazantzi AK, Vamvatsikos D (2015) Intensity measure selection for vulnerability studies of building classes. *Earthq Eng Struct Dyn* 44(15):2677–2694. <https://doi.org/10.1002/eqe.2603>
- Kohrangi M, Vamvatsikos D, Bazzurro P (2016) Implications of intensity measure selection for seismic loss assessment of 3-D buildings. *Earthq Spectra* 32(4):2167–2189. <https://doi.org/10.1193/112215EQS177M>
- Kohrangi M, Bazzurro P, Vamvatsikos D, Spillatura A (2017) Conditional spectrum-based ground motion record selection using average spectral acceleration. *Earthq Eng Struct Dyn* 46(10):1667–1685. <https://doi.org/10.1002/eqe.2876>
- Lagomarsino S, Giovinazzi S (2006) Macroseismic and mechanical models for the vulnerability and damage assessment of current buildings. *Bull Earthq Eng* 4(4):415–443. <https://doi.org/10.1007/s10518-006-9024-z>

- Lin T, Haselton CB, Baker JW (2013) Conditional spectrum-based ground motion selection. Part II: intensity-based assessments and evaluation of alternative target spectra. *Earthq Eng Struct Dyn* 42(12):1867–1884. <https://doi.org/10.1002/eqe.2303>
- Luco N, Bazzurro P (2007) Does amplitude scaling of ground motion records result in biased nonlinear structural drift responses? *Earthq Eng Struct Dyn* 36(13):1813–1835. <https://doi.org/10.1002/eqe.695>
- McKenna F, Scott MH, Fenves GL (2010) Nonlinear finite-element analysis software architecture using object composition. *J Comput Civ Eng* 24(1):95–107. [https://doi.org/10.1061/\(ASCE\)CP.1943-5487.0000002](https://doi.org/10.1061/(ASCE)CP.1943-5487.0000002)
- Mehanny SSF (2009) A broad-range power-law form scalar-based seismic intensity measure. *Eng Struct* 31(7):1354–1368. <https://doi.org/10.1016/j.engstruct.2009.02.003>
- Minas S, Galasso C (2019) Accounting for spectral shape in simplified fragility analysis of case-study reinforced concrete frames. *Soil Dyn Earthq Eng* 119(April):91–103. <https://doi.org/10.1016/j.soildyn.2018.12.025>
- Morandi P, Hak S, Magenes G (2018) Mechanical characterization and force-displacement hysteretic curves from in-plane cyclic tests on strong Masonry Infills. *Data Brief* 16(February):886–904. <https://doi.org/10.1016/j.dib.2017.12.015>
- Nafeh AMB, O'Reilly GJ, Monteiro R (2020) Simplified seismic assessment of infilled RC frame structures. *Bull Earthq Eng* 18(4):1579–1611. <https://doi.org/10.1007/s10518-019-00758-2>
- O'Reilly GJ, Sullivan TJ (2018a) Probabilistic seismic assessment and retrofit considerations for Italian RC frame buildings. *Bull Earthq Eng* 16(3):1447–1485. <https://doi.org/10.1007/s10518-017-0257-9>
- O'Reilly GJ, Sullivan TJ (2018b) Quantification of modelling uncertainty in existing Italian RC frames. *Earthq Eng Struct Dyn* 47(4):1054–1074. <https://doi.org/10.1002/eqe.3005>
- O'Reilly GJ, Monteiro R (2019) Probabilistic models for structures with bilinear demand-intensity relationships. *Earthq Eng Struct Dyn* 48(2):253–268. <https://doi.org/10.1002/eqe.3135>
- O'Reilly GJ, Sullivan TJ (2019) Modeling techniques for the seismic assessment of the existing Italian RC frame Structures. *J Earthquake Eng* 23(8):1262–1296. <https://doi.org/10.1080/13632469.2017.1360224>
- O'Reilly GJ, Kohrangi M, Bazzurro P, Monteiro R (2018a) Intensity measures for the collapse assessment of infilled RC frames. In: 16th European conference on earthquake engineering. Thessaloniki, Greece
- O'Reilly GJ, Perrone D, Fox M, Monteiro R, Filiatrault A (2018b) Seismic assessment and loss estimation of existing school buildings in Italy. *Eng Struct* 168 (August):142–162. <https://doi.org/10.1016/j.engstruct.2018.04.056>
- O'Reilly GJ, Sullivan TJ, Monteiro R (2018c) On the seismic assessment and retrofit of infilled RC frames structures. In: 16th European conference on earthquake engineering. Thessaloniki, Greece
- O'Reilly GJ, Perrone D, Fox M, Monteiro R, Filiatrault A, Lanese I, Pavese A (2019) System identification and seismic assessment modeling implications for Italian school buildings. *J Perform Constr Facil* 33(1):04018089. [https://doi.org/10.1061/\(ASCE\)CF.1943-5509.0001237](https://doi.org/10.1061/(ASCE)CF.1943-5509.0001237)
- Padgett JE, Nielson BG, DesRoches R (2008) Selection of optimal intensity measures in probabilistic seismic demand models of highway bridge portfolios. *Earthq Eng Struct Dyn* 37(5):711–725. <https://doi.org/10.1002/eqe.782>
- Ricci P, De Luca F, Verderame GM (2011) 6th April 2009 L'Aquila earthquake, Italy: reinforced concrete building performance. *Bull Earthq Eng* 9(1):285–305. <https://doi.org/10.1007/s10518-010-9204-8>
- Rossetto T, Elnashai A (2003) Derivation of vulnerability functions for European-type RC structures based on observational data. *Eng Struct* 25(10):1241–1263. [https://doi.org/10.1016/S0141-0296\(03\)00060-9](https://doi.org/10.1016/S0141-0296(03)00060-9)
- Rota M, Penna A, Strobbia CL (2008) Processing Italian damage data to derive typological fragility curves. *Soil Dyn Earthq Eng* 28(10–11):933–947. <https://doi.org/10.1016/j.soildyn.2007.10.010>
- Sassun K, Sullivan TJ, Morandi P, Cardone D (2015) Characterising the in-plane seismic performance of infill masonry. *Bull N Z Soc Earthq Eng* 49(1):100–117
- Silva V, Casotto C, Rao A, Villar M, Crowley H, Vamvatsikos D (2015) OpenQuake Risk Modeller's Toolkit—User Guide. 2015–09. <https://doi.org/10.13117/GEM.OPENQUAKE.MAN.RMTK.1.0>
- Silva V, Akkar S, Baker J, Bazzurro P, Castro JM, Crowley H, Dolsek M et al (2019) Current challenges and future trends in analytical fragility and vulnerability modeling. *Earthq Spectra* 35(4):1927–1952. <https://doi.org/10.1193/042418EQS1010>
- Song B, Galasso C, Kanvinde A (2020) Advancing fracture fragility assessment of pre-northridge welded column splices. *Earthq Eng Struct Dyn* 49(2):132–154. <https://doi.org/10.1002/eqe.3228>
- Sousa L, Silva V, Marques M, Crowley H (2016) On the treatment of uncertainties in the development of fragility functions for earthquake loss estimation of building portfolios. *Earthq Eng Struct Dyn*. <https://doi.org/10.1002/eqe.2734>
- Trifunac MD, Brady AG (1975) A study on the duration of strong earthquake ground motion. *Bull Seismol Soc Am* 65(3):581–626

- Vamvatsikos D, Allin Cornell C (2002) Incremental dynamic analysis. *Earthq Eng Struct Dyn* 31(3):491–514. <https://doi.org/10.1002/eqe.141>
- Vamvatsikos D, Allin Cornell C (2004) Applied incremental dynamic analysis. *Earthq Spectra* 20(2):523–553. <https://doi.org/10.1193/1.1737737>
- Villar-Vega M, Silva V, Crowley H, Yepes C, Tarque N, Acevedo AB, Hube MA, Gustavo CD, María HS (2017) Development of a fragility model for the residential building stock in South America. *Earthq Spectra* 33(2):581–604. <https://doi.org/10.1193/010716EQS005M>
- Woessner J, Laurentiu D, Giardini D, Crowley H, Cotton F, Grünthal G, Valensise G et al (2015) The 2013 European seismic hazard model: key components and results. *Bull Earthq Eng* 13(12):3553–3596. <https://doi.org/10.1007/s10518-015-9795-1>

Publisher's Note Springer Nature remains neutral with regard to jurisdictional claims in published maps and institutional affiliations.